Plant Physiol. (1998) 116: 271–278

# Symplasmic Constriction and Ultrastructural Features of the Sieve Element/Companion Cell Complex in the Transport Phloem of Apoplasmically and Symplasmically Phloem-Loading Species[1]

**Ronald Kempers*, Ankie Ammerlaan, and Aart J.E. van Bel**

Transport Physiology Research Group, Department of Plant Ecology and Evolutionary Biology, Utrecht University, Sorbonnelaan 16, NL-3584 CA Utrecht, The Netherlands (R.K., A.A.); and Institut für Allgemeine Botanik und Pflanzenphysiologie, Justus-Liebig Universität Giessen, Senckenbergstrasse 17, D-35390 Giessen, Germany (A.J.E.v.B.)

**The ultrastructural features of the sieve element/companion cell complexes were screened in the stem phloem of two symplasmically loading (squash, [*Cucurbita maxima* L.] and *Lythrum salicaria* L.) and two apoplasmically loading (broad bean [*Vicia faba* L.] and *Zinnia elegans* L.) species. The distinct ultrastructural differences between the companion cells in the collection phloem of symplasmically and apoplasmically phloem-loading species continue to exist in the transport phloem. Plasmodesmograms of the stem phloem showed a universal symplasmic constriction at the interface between the sieve element/companion cell complex and the phloem parenchyma cells. This contrasts with the huge variation in symplasmic continuity between companion cells and adjoining cells in the collection phloem of symplasmically and apoplasmically loading species. Further, the ultrastructure of the companion cells in the transport phloem faintly reflected the features of the companion cells in the loading zone of the transport phloem. The companion cells of squash contained numerous small vacuoles (or vesicles), and those of *L. salicaria* contained a limited number of vacuoles. The companion cells of broad bean and *Z. elegans* possessed small wall protrusions. Implications of the present findings for carbohydrate processing in intact plants are discussed.**

In the leaves of dicotyledons two modes of phloem loading have been identified (Turgeon and Wimmers, 1988; van Bel et al., 1992, 1994). These mechanisms of phloem loading, symplasmic or apoplasmic, seem to be associated with minor vein configuration (Gamalei, 1985, 1989) and carbohydrate metabolism (Gamalei, 1985; Turgeon et al., 1993; Flora and Madore, 1996). CCs in minor veins of apoplasmically phloem-loading species (further referred to as apoplasmic species) are termed TCs and have virtually no plasmodesmata at the interface with the mesophyll domains (Gamalei, 1989). The TCs possess cell wall protrusions, varying in surface area with the transit of photosynthate, and unfragmented vacuoles (Gamalei, 1989; Wimmers and Turgeon, 1991; Gamalei et al., 1992). CCs in minor veins of symplasmically phloem-loading species (further referred to as symplasmic species) are termed ICs and are connected with the mesophyll symplast via numerous plasmodesmata (Gamalei, 1989). The ICs usually contain vesicular networks or heavily fragmented vacuoles and have no cell wall protrusions (Gamalei, 1989).

The most persuasive evidence for two phloem-loading mechanisms is the consistent coincidence between physiological behavior and minor vein configuration. The diverse structure-functional indications in favor of two modes of phloem loading are numerous and were thoroughly reviewed by van Bel (1996). More recent evidence supports the existence of principally different systems of phloem loading (Flora and Madore, 1996; Kingston-Smith and Pollock, 1996).

The question arises whether the different ways of carbohydrate processing in the phloem-loading zone continue to exist along the phloem trajectory, of which ultrastructure and plasmodesmal connectivity of the CCs in the transport phloem may be indicative. Hence, the present electron-microscopic investigation was focused on the ultrastructure of the CCs in the transport phloem of two species that were described to be symplasmic, squash (*Cucurbita maxima* L.; Gamalei, 1991) and *Lythrum salicaria* L. (van Bel et al., 1994), and two species that were considered to be apoplasmic, broad bean (*Vicia faba* L.; Gamalei, 1991) and *Zinnia elegans* L. (Y.V. Gamalei and A.V. Sjutkina, unpublished results), to obtain an impression of the functional continuity between collection and transport phloem in apoplasmic and symplasmic loaders.

## MATERIALS AND METHODS

Phloem specimens were cut from the stems of four species, broad bean (*Vicia faba* L. cv Witkiem major [Nunhems Zaden bv, Haelen, The Netherlands]), *Lythrum salicaria* L., *Zinnia elegans* L. (bv Cruydthoeck, Groningen, The Netherlands), and squash (*Cucurbita maxima* L. cv Golden Deli-

[1] A part of this study was subsidized by NWO (Dutch Organization for Scientific Research).

* Corresponding author; e-mail r.kempers@boev.biol.ruu.nl; fax 31–30–251–8366.

Abbreviations: CC, companion cell; IC, intermediary cell; PP, phloem parenchyma cell; PPU, pore/plasmodesma unit; SE/CC, sieve element; TC, transfer cell.

cious [Botanical Garden, Utrecht University, The Netherlands]), and from the leaves of *L. salicaria* and *Z. elegans*. All plants were grown under standard greenhouse conditions: 25°C; 70% RH; 14-h day/10-h night period; and illumination, daylight plus additional lamp light (HPI-T 400 W; Philips, Eindhoven, The Netherlands) up to a minimum irradiance of 250 $\mu$mol photons $m^{-2}$ $s^{-1}$ at plant level. Plants between 4 and 8 weeks old, depending on the species, were used just before flowering.

### Electron Microscopy

Pieces (3 $mm^3$) were cut from the phloem region of fully extended internodes in 10 mL of fixative (50 mol $m^{-3}$ sodium cacodylate buffer, 2 mol $m^{-3}$ $CaCl_2$, and 5% [v/v] glutaraldehyde, pH 7.0). The pieces were rinsed in fresh fixative at room temperature and placed under a low vacuum to remove the air from the intercellular spaces, which facilitated the entrance of the fixative into the tissue. A similar fixation procedure was followed for pieces of mature leaves (4 $mm^2$) of *L. salicaria* and *Z. elegans*. The total fixation time was approximately 7 h with a replacement of the fixative after 1 h. Subsequently, the pieces were rinsed in buffer (50 mol $m^{-3}$ sodium cacodylate buffer, pH 7.0) and postfixed overnight at 4°C in 2% (w/v) $OsO_4$ (in sodium cacodylate buffer). After the pieces were rinsed thoroughly in buffer, dehydration was performed using a graded ethanol series followed by embedding in Spurr's resin. Ultrathin sections (60–80 nm) were cut with a diamond knife on an OM-U3 ultramicrotome (Reichert, Vienna, Austria), mounted on copper thin-bar grids (200 mesh) coated with Formvar film, stained with uranyl acetate/lead citrate, and photographed in an EM 10 transmission electron microscope (Zeiss).

### Determination of Plasmodesmal Densities and Frequencies

Five series of ultrathin, transverse sections were cut from the secondary phloem area of the stem tissue of every species. Each series was cut at a distance of approximately 20 $\mu$m from the previous one (to overcome the effect of potential plasmodesmal clustering) and consisted of 30 randomly picked ultrathin sections. From each series a few semithin sections were cut for light microscopy to produce a topographical map of the phloem area. For each series, 10 cell complexes (consisting of SE, CC, and PP) were spotted, marked on the topographical map, and followed through the serial section sequence. In a total of 150 sections per species (five series consisting of 30 sections each), 50 cell complexes (five series consisting of 10 cell complexes) were investigated for plasmodesmal connections. Plasmodesmata were counted at all cell interfaces (i.e. SE/CC, SE/PP, CC/PP, and PP/PP) within the marked complexes. For *L. salicaria* and *Z. elegans*, transverse sections of the minor veins were prepared and the plasmodesmal frequency between the mesophyll and the CCs was determined according to the method of Gamalei (1991). Only those plasmodesmata that stretched further than the primary cell wall were scored. All branched plasmodesmata, either branching at one end or at both ends, were scored as one. The quantitation of the plasmodesmal occurrence was based on countings of radially and tangentially oriented plasmodesmata and not on longitudinal ones. Section thickness was kept as constant as possible and varied between 60 and 80 nm.

The lengths of the respective cell-cell interfaces were determined with a curvimeter (no. 708200, Freiberger Präzisionmechanik, Freiburg, Germany) on electron micrographs. The results of the plasmodesmal counting are given as the number of plasmodesmata per micrometer of specific cell-cell contact interface length, referred to as plasmodesmal density, and as the total number of plasmodesmata per contact site per micrometer of sieve tube length, referred to as plasmodesmal frequency (Botha and van Bel, 1992).

## RESULTS

### General Ultrastructural Features of the Transport Phloem

The secondary phloem of the investigated species consisted of the constitution that has been described as "regular" for dicotyledons (Esau, 1969). In the case of *C. maxima*, only the external phloem of the bicollateral vascular bundles was studied. The plasmodesmal contacts between the PPs were generally clustered in pit fields, unbranched with a median cavity, and ultrastructurally similar to those reported by Esau (1969). The characteristic intercellular contacts at the SE/CC interface (termed PPUs; van Bel and Kempers, 1996) are composed of branching plasmodesmata at the CC side that converge into a single (sometimes enlarged) pore at the SE side (Wooding and Northcote, 1965; Esau and Thorsch, 1985; Evert, 1990). The scarce plasmodesmata between the CC and PP were not clustered and ultrastructurally similar to those between the PPs with an occasional branching at the CC side. The plasmodesmal contacts between consecutive CCs in *C. maxima* had a characteristic multifurcating appearance that radiated from the middle lamella toward both cells (Fig. 1A). The extremely rare plasmodesmata encountered at the SE/PP boundary were single and unbranched.

### Ultrastructure of the SE/CC Complexes of the Transport Phloem

#### *C. maxima*

No cell wall protrusions were present in the CCs, which had a diameter of 6.4 ± 1.9 $\mu$m (Table I). The CCs possessed a dense cytoplasm with a mass of fragmented vacuoles (or ER vesicles) of various sizes, ranging from less than 0.1 $\mu$m to several micrometers (Fig. 2A). The SEs had a diameter of 9.8 ± 5.5 $\mu$m (Table I) and generally contained thick secondary walls, which were thinner or absent around the PPU pores.

#### *L. salicaria*

The CCs of *L. salicaria* did not possess any cell wall protrusions (Fig. 2B) and had an average diameter of 4.1 ±

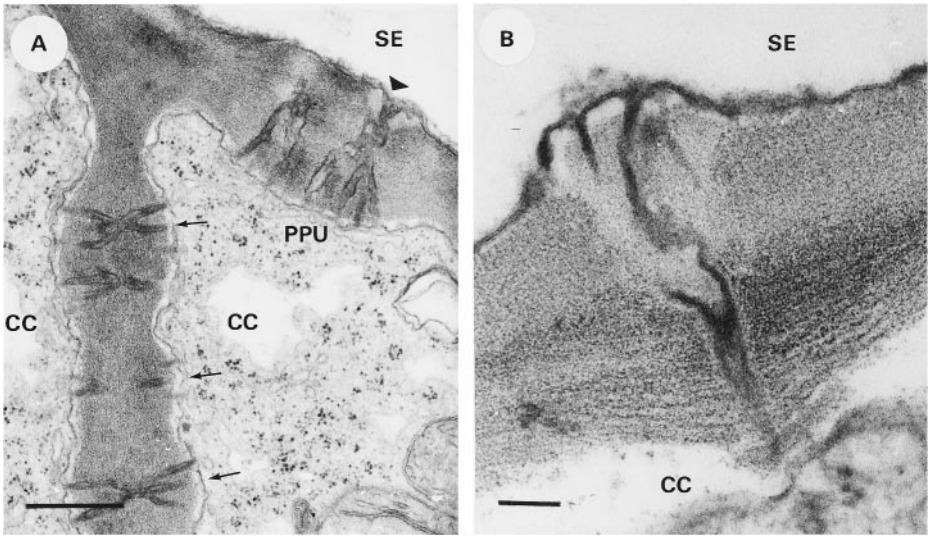


**Figure 1.** Different types of plasmodesmata in the transport phloem. A, *C. maxima*; plasmodesmata between the SE and CC (PPUs) and between the CCs. In the PPUs a single pore on the SE side (arrowhead) is jointed with the plasmodesmal branches on the CC side, which resemble the plasmodesmal branches (arrows) between the CCs. B, *Z. elegans*; in contrast to the usual orientation, the PPU appears to have the furcating plasmodesmata at the SE side and the single pore end to the CC side. Bar: A, 0.5 μm; B, 100 nm.

1.3 μm (Table I). The vacuole of the CCs was fragmented to some degree (vacuole diameters varying from 0.1 μm to several micrometers). The PPUs had a variable number of branches and small mounds of wall material at the CC side. The SEs had a diameter of 5.8 ± 1.0 μm (Table I), and the inner side of the SE plasma membrane appeared to be covered with an electron-dense material, which was also observed near the pore end of the PPU (Fig. 2B).

### *V. faba*

In accordance with an earlier observation (Couot-Gastelier, 1982), distinct cell wall protrusions were observed in the CCs of *V. faba* except at the cell wall interface between the CC and SE. The diameter of the CCs was 6.2 ± 1.4 μm (Table I). The very dense cytoplasm had a fine, granular structure (Fig. 2C). The vacuole was not fragmented but occasionally had a lobed appearance. The SEs had a diameter of 9.3 ± 1.3 μm (Table I) and a dark lining of the plasma membrane was visible at the lumen side of the SE (Fig. 2C).

### *Z. elegans*

The CCs of *Z. elegans* (Fig. 2D) possessed cell wall protrusions that were not as marked and regularly shaped as those of the CCs of *V. faba*. The cytoplasm of the CCs had a granular appearance with some osmiophilic globules and a generally unfragmented, slightly lobed vacuole (Fig. 2D). The CC diameter was 3.7 ± 1.0 μm (Table I). The seemingly reverse orientation of some PPUs (the furcating end toward the SE; Fig. 1B) was a remarkable feature. Although no significant ultrastructural differences between these PPUs and the normally positioned PPUs in the same tissue were found, the seemingly reverse orientation may be the result of an oblique section through a normally positioned PPU. The SEs had a diameter of 5.7 ± 1.9 μm (Table I) and contained some membranous material in the lumen.

## Comparative Plasmodesmograms Based on the Plasmodesmal Density and on the Plasmodesmal Frequency

Plasmodesmal densities and frequencies are numerical parameters that show the potential for symplasmic transport between cells. Setting aside the question of whether the observed plasmodesmata are functional or not, it is important how the plasmodesmal connectivity is defined (Fisher, 1990; van Bel and Oparka, 1995). In this study plasmodesmal numbers are expressed according to the

**Table I.** *Comparison of the diameters of CCs and SEs and their ratio in the collection and the transport phloem*

| Phloem Type | *C. maxima* | | | *L. salicaria* | | | *V. faba* | | | *Z. elegans* | | |
|---|---|---|---|---|---|---|---|---|---|---|---|---|
| | CC | SE | CC/SE | CC | SE | CC/SE | CC | SE | CC/SE | CC | SE | CC/SE |
| | μm | | | | | | | | | | | |
| Collection | 12.5[a] | 3.5[a] | 3.6 | 5.0 | 1.6 | 3.1 | 12.5[b] | 4.5[b] | 2.8 | 5.5 | 1.8 | 3.0 |
| Transport | 6.4 | 9.8 | 0.65 | 4.1 | 5.5 | 0.7 | 6.2 | 9.3 | 0.7 | 3.7 | 5.7 | 0.65 |

[a] After Turgeon et al. (1975) and Schmitz et al. (1987). [b] After Gunning et al. (1974).

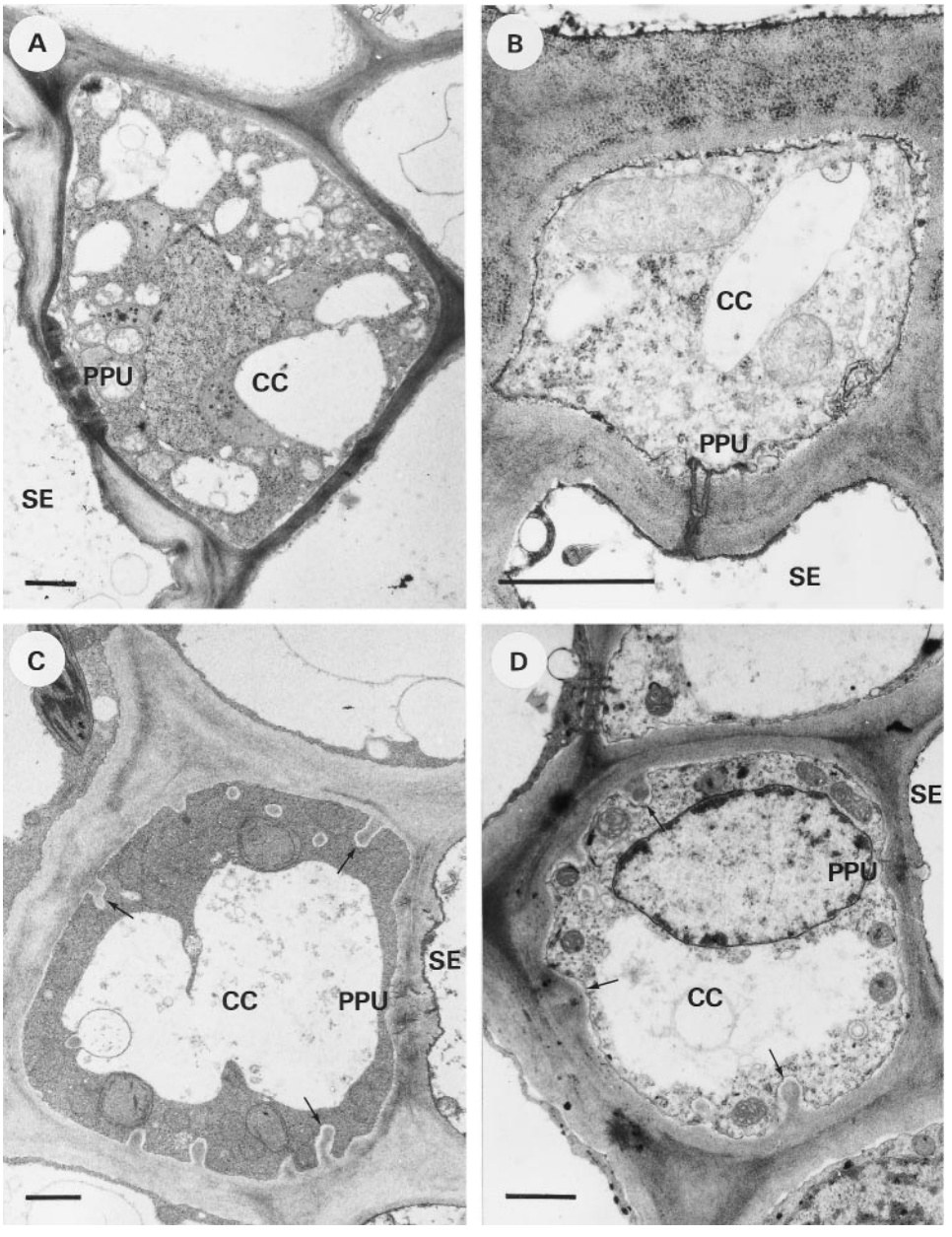


**Figure 2.** Transverse sections of CCs in the transport phloem. A, *C. maxima*; the dense cytoplasm contains many small vacuoles or vesicles. B, *L. salicaria*; a fragmented vacuole is present. C, *V. faba*; cell wall protrusions (arrows) occur on all sides except at the SE/CC interface. The vacuole is unfragmented. D, *Z. elegans*; small cell wall protrusions (arrows) occur on all sides except at the SE/CC interface. Bars = 1 $\mu$m.

method of Botha and van Bel (1992), i.e. as plasmodesmal density and plasmodesmal frequency (for definitions, see "Materials and Methods"). The absolute numbers of plasmodesmata for density and frequency are to be used for interspecific comparison, and the proportional (percentual) distributions are useful for intraspecific comparison (Fig. 3).

The data clearly indicate (Fig. 3) that the highest plasmodesmal densities and frequencies are associated with the PP/PP interfaces in all of the species that we investigated, with a maximum plasmodesmal frequency of 12.350 plasmodesmata $\mu m^{-1}$ sieve tube length (76.5%) for *V. faba*. By contrast, there is practically no plasmodesmal connectivity in any of the species between PP and SE (Fig. 3B). Plasmodesmal frequencies between CC and PP are higher than those at the SE/PP interfaces, with the highest value of 2.125 plasmodesmata $\mu m^{-1}$ sieve tube length (11%) in *C. maxima* (Fig. 3B). The smallest plasmodesmal frequency at the CC/PP interface was found in *L. salicaria* (Fig. 3B), being 0.250 plasmodesmata $\mu m^{-1}$ sieve tube length (2.0%). The data collectively show a constriction in the symplasmic

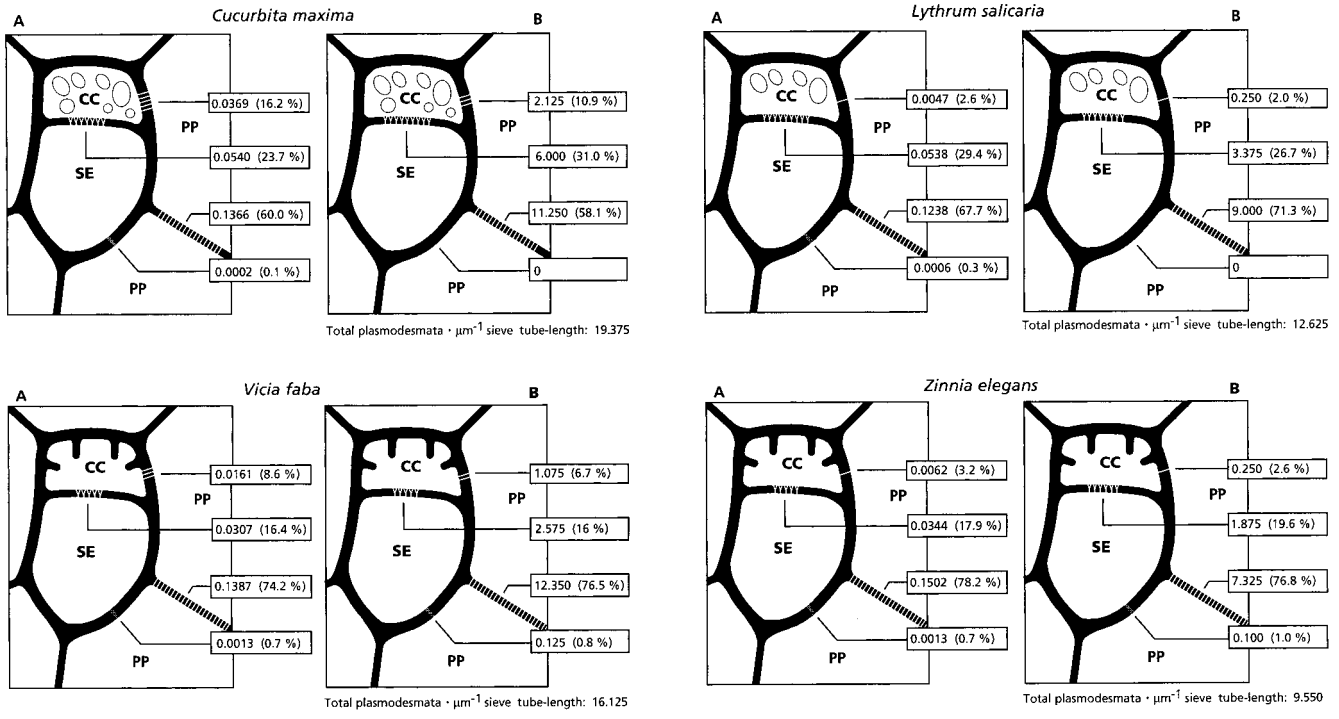


**Figure 3.** Plasmodesmograms representing the plasmodesmal densities in the A plots (expressed as the number of plasmodesmata per micrometer of cell wall interface length). The B plots represent the plasmodesmal frequency (expressed as the total number of plasmodesmata per micrometer of sieve tube length). The two symplasmic species are located in the upper part of the figure and show fragmented vacuoles (or vesicles) in the CCs as a typical ultrastructural feature. The two apoplasmic species are in the lower part of the figure and have cell wall protrusions as a typical ultrastructural feature. The absolute numbers of plasmodesmata enable interspecific comparison of plasmodesmal occurrence at the respective interfaces. The proportional distributions (given as percentages in parentheses) are represented by the striping between the respective cell types and enable intraspecific comparison (Fisher, 1990; Botha and van Bel, 1992).

passageway between the SE/CC complex and the PPs in all species investigated.

### Ultrastructural Features and Plasmodesmal Frequencies of the Collection Phloem of *L. salicaria* and *Z. elegans*

The ICs in the minor veins of *L. salicaria* did not possess any cell wall protrusions (Fig. 4A). Their average diameter was 5.0 ± 0.9 µm (Table I). The vacuole was fragmented into two or three subvacuoles and the cytoplasm was not very dense. The SEs had an average diameter of 1.6 ± 0.9 µm (Table I). The plasmodesmal frequency at the interface between the CCs and the mesophyll was determined, according to the method of Gamalei (1991), to be 1.27 plasmodesmata $\mu m^{-2}$ (Table II).

In the minor veins of *Z. elegans* prominent cell wall protrusions were observed in the TCs (Fig. 4B). The TCs, with an average diameter of 5.5 ± 1.9 µm (Table I), had an unfragmented vacuole and a very dense cytoplasm. The SEs had an average diameter of 1.8 ± 0.8 µm (Table I). The plasmodesmal frequency at the interface between the CCs and the mesophyll was determined, according to the method of Gamalei (1991), to be 0.04 plasmodesmata $\mu m^{-2}$ (Table II).

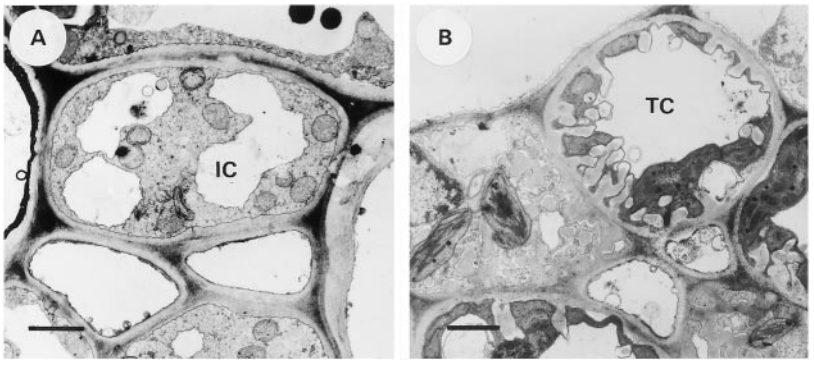


**Figure 4.** Transverse sections of the CCs in the minor veins of the collection phloem. A, *L. salicaria*; an IC with limited vacuolization. B, *Z. elegans*; a TC with distinct cell wall protrusions and an unfragmented vacuole. Bars = 1 µm.

**Table II.** *Plasmodesmal frequencies between CCs and the adjoining mesophyll in the minor veins of the collection phloem*

| Species | CC/Mesophyll Interface |
|---|---|
| | *no. plasmodesmata* $\mu m^{-2}$ |
| *C. maxima* | 48.16[a] |
| *L. salicaria* | 1.27 |
| *V. faba* | 0.07[a] |
| *Z. elegans* | 0.04 |

[a] After Gamalei (1991).

## DISCUSSION

### Comparison of the CC Ultrastructure in Collection and Transport Phloem

In the investigated species with ICs in the collection phloem, the CCs in the transport phloem also contain fragmented vacuoles (or vesicles). In the investigated species with TCs in the collection phloem, the CCs in the transport phloem also possess cell wall protrusions. The characteristic ultrastructural differences between the CCs of the collection phloem in symplasmic and apoplasmic species (Gamalei, 1989) thus appear to continue, although less distinctly, in the transport phloem (Fig. 2). The one exception is a dramatic reduction of the plasmodesmal frequencies between the SE/CC complex and the adjoining PPs in the transport phloem of symplasmic species (Fig. 3B). The relative uniformity of the plasmodesmal frequencies in the transport phloem contrasts with their high quantitative variation in the collection phloem (Fig. 4; Table II). In both symplasmic and apoplasmic species, the absolute diameter of the CCs in the transport phloem was smaller and proportional to the SEs (Table I). In all species the SE/CC-diameter ratio in the collection phloem was invariably higher than in the transport phloem (Table I).

The fragmented vacuoles or vesicles, characteristic of the IC ultrastructure in cucurbits (Turgeon et al., 1975; Schmitz et al., 1987; Gamalei, 1989) and presumably involved in symplasmic carbohydrate processing (Gamalei et al., 1994), were also observed in the CCs of the transport phloem of *C. maxima* (Fig. 2A) and *L. salicaria* (Fig. 2B). The number of vesicles in the CCs of *L. salicaria* was close to that in the ICs (Fig. 4B). Its physical behavior in response to parachloromercuribenzenesulfonic acid (van Bel et al., 1994) excluded the possibility that *L. salicaria* is an apoplasmic species, but it may not be an articulate symplasmic species for a few reasons. The plasmodesmal frequencies at the CC/mesophyll interface in *L. salicaria* lies between those of distinct symplasmic and apoplasmic species (Gamalei, 1991). This, in combination with the low number of vesicles, suggests that the CCs in the collection phloem of *L. salicaria* have "smooth-walled" traits (Turgeon, 1996).

The cell wall protrusions characteristic of the TC ultrastructure in minor veins and indicative of apoplasmic phloem loading (Gamalei, 1989; Wimmers and Turgeon, 1991) also occur in the CCs of transport phloem of *V. faba* and *Z. elegans* (Fig. 2, C and D). Yet, the cell wall protrusions in the CCs of the transport phloem were considerably smaller than those in the collection phloem of *V. faba* (Gunning et al., 1974); Fig. 2C) and *Z. elegans* (Figs. 2D and 4B). The protrusions in the CCs of the transport phloem were absent at the side adjacent to the SE. This renders credence to the idea that the CCs play an important role in retrieval of solutes leaking away from the SE/CC complexes in the transport phloem (van Bel, 1996).

### Plasmodesmal Frequencies in the Transport Phloem

Decisive for transport and communication between cells is the collective diameter of the symplasmic corridors (deducible from the plasmodesmal frequency) and not the corridor density. On the other hand, the plasmodesmal density is indicative of the exchange intensity at certain interfaces. Therefore, both ways of expressing plasmodesmal connectivity have been presented.

The plasmodesmal frequencies and densities between the PPs of the transport phloem are remarkably constant between the species, with those in *C. maxima* being the lowest (Fig. 3). In turn, the plasmodesmal connectivity between CC and PP is the highest in *C. maxima* (Fig. 3). As for the plasmodesmal connectivity between the CC and PP, the overall picture is confusing. The plasmodesmal frequencies between the CC and PP are uniformly low, but there is no clear demarcation between the symplasmic and apoplasmic species (Fig. 3B). Noteworthy are the differences between the symplasmic and the apoplasmic species at the interfaces between the SE-PP and the SE-CC (Fig. 3). Minor symplasmic continuity does exist between the PP and the SE but only in the investigated apoplasmic species. Furthermore, the plasmodesmal frequency between the CC and the SE is higher in the apoplasmic species described here (Fig. 3B).

### The Physiological Significance of the Symplasmic Constriction between the SE/CC Complex and the Phloem Parenchyma in Transport Phloem

The symplasmic constriction between the SE/CC complex and the PPs in the transport phloem has been identified before in bean (*Phaseolus vulgaris*; Hayes et al., 1985) and castor bean (*Ricinus communis;* van Bel and Kempers, 1991) stems. The question arises whether the numerical constriction also presents a physiological bottleneck. A relationship between the frequencies and the size of the passageway hinges on the molecular exclusion limit and the gating status of the plasmodesmata.

The symplasmic continuity between the SE/CC complex and the adjoining PPs in transport phloem has been clearly shown by various approaches in a number of species (for reviews, see van Bel, 1996; van Bel and Kempers, 1996). In contrast to these indications for symplasmic discontinuity, other experiments indicate a reversible and controlled gating of the plasmodesmata between the SE/CC complexes and the PPs (Hayes et al., 1987; Patrick and Offler, 1996; Wright and Oparka, 1997). In stems of summer-grown bean plants, photosynthate appeared to move symplasmically from the sieve tubes to the surrounding tissues, whereas photosynthate was apoplasmically released in winter-grown plants (Hayes et al., 1987). The different pathways

of photosynthate release from transport phloem have recently been substantiated by experiments with 5(6)carboxyfluorescein diacetate (Patrick and Offler, 1996). Supplementary experiments with Arabidopsis seedlings showed that CFDA moved out of the transport phloem while this was being treated with metabolic inhibitors (Wright and Oparka, 1997). This phenomenon is consistent with the observation that metabolic inhibitors open up plasmodesmata and thus allow a higher degree of symplasmic exchange (Tucker, 1993; Cleland et al., 1994).

How are these paradoxical results of symplasmic continuity explained? The plasmodesmata at the CC/PP interface, which present a symplasmic bottleneck, may close completely in response to injury. Because the majority of experiments favoring a symplasmic isolation of the SE/CC complexes has been done with tissue slices, the damage inflicted may have effected a complete isolation of the SE/CC complexes (Van der Schoot and van Bel, 1989; van Bel and Kempers, 1991; Oparka et al., 1992; van Bel and Van Rijen, 1994; Kempers and van Bel, 1997). In intact plants the few plasmodesmata that make up the symplasmic constriction between the CC and the PP may be open (Hayes et al., 1987; Patrick and Offler, 1996; Wright and Oparka, 1997) or closed (Oparka et al., 1994, 1995; Rhodes et al., 1996).

## ACKNOWLEDGMENTS

The authors gratefully acknowledge Prof. Y.V. Gamalei and Dr. A.V. Sjutkina (Komarov Botanical Institute, St. Petersburg, Russia) for the determination of the plasmodesmal frequency in the leaf of *Z elegans*. M. Geels (Department of Image Processing and Design, Utrecht University, The Netherlands) is thanked for technical assistance with preparing of the plasmodesmograms.

Received May 29, 1997; accepted September 16, 1997.


## LITERATURE CITED

**Botha CEJ, van Bel AJE** (1992) Quantification of symplastic continuity as visualised by plasmodesmograms: diagnostic value for phloem-loading pathways. Planta **187:** 359–366

**Cleland RE, Fujiwara T, Lucas WJ** (1994) Plasmodesmal-mediated cell-to-cell transport in wheat roots is modulated by anaerobic stress. Protoplasma **178:** 81–85

**Couot-Gastelier J** (1982) Particularités fonctionnelles et infrastructurales du tissu phloémien du *Vicia faba* L. Beitr Biol Pflanz **57:** 257–268

**Esau K** (1969) The Phloem. *In* W Zimmermann, P Ozenda, HD Wulff, eds, Encyclopedia of Plant Anatomy, Vol 5. Borntraeger, Berlin

**Esau K, Thorsch J** (1985) Sieve plate pores and plasmodesmata, the communication channels of the symplast: ultrastructural aspects and developmental relations. Am J Bot **72:** 1641–1653

**Evert RF** (1990) Dicotyledons. *In* H-D Behnke, RD Sjölund, eds, Sieve Elements. Comparative Structure, Induction and Development. Springer-Verlag, Berlin, pp 103–137

**Fisher DG** (1990) Distribution of plasmodesmata in leaves. A comparison of *Cananga odorata* with other species using different measures of plasmodesmatal frequency. *In* AW Robards, WJ Lucas, JD Pitts, HJ Jongsma, DC Spray, eds, Proceedings of the NATO Advanced Workshop: Parallels in Cell to Cell Junctions in Plants and Animals. Springer-Verlag, Berlin, pp 199–221

**Flora LL, Madore MA** (1996) Significance of minor-vein anatomy to carbohydrate transport. Planta **198:** 171–178

**Gamalei Y** (1989) Structure and function of leaf minor veins in trees and herbs. Trees **3:** 96–110

**Gamalei Y** (1991) Phloem loading and its development related to plant evolution from trees to herbs. Trees **5:** 50–64

**Gamalei YV** (1985) Characteristics of phloem loading in woody and herbaceous plants. Fiziol Rast **32:** 866–875

**Gamalei YV, Pakhomova MV, Sjutkina AV** (1992) Ecological aspects of assimilate transport. I. Temperature. Fiziol Rast **39:** 1068–1078

**Gamalei YV, van Bel AJE, Pakhomova MV, Sjutkina AV** (1994) Effects of temperature on the conformation of the endoplasmic reticulum and on starch accumulation in leaves with the symplasmic minor-vein configuration. Planta **194:** 443–453

**Gunning BES, Pate JS, Minchin FR, Marks I** (1974) Quantitative aspects of transfer cell structure in relation to vein loading in leaves and solute transport in legume nodules. *In* MA Sleigh, DH Jennings, eds, Transport at the Cellular Level. Cambridge University Press, Cambridge, UK, pp 87–125

**Hayes PM, Offler CE, Patrick JW** (1985) Cellular structures, plasma membrane surface areas and plasmodesmatal frequencies of the stem of *Phaseolus vulgaris* L. in relation to radial photosynthate transfer. Ann Bot **56:** 125–138

**Hayes PM, Patrick JW, Offler CE** (1987) The cellular pathway of radial transfer in stems of *Phaseolus vulgaris* L.: effects of cellular plasmolysis and p-chloromercuribenzene-sulphonic acid. Ann Bot **59:** 635–642

**Kempers R, van Bel AJE** (1997) Symplasmic connections between sieve element and companion cell in the stem phloem of *Vicia faba* L. have a molecular exclusion limit of at least 10 kDa. Planta **201:** 195–201

**Kingston-Smith AH, Pollock CJ** (1996) Tissue level localization of acid invertase in leaves: an hypothesis for the regulation of carbon export. New Phytol **134:** 423–432

**Oparka KJ, Duckett CM, Prior DAM, Fisher DB** (1994) Real-time imaging of phloem unloading in the root tip of *Arabidopsis*. Plant J **6:** 759–766

**Oparka KJ, Prior DAM, Wright KM** (1995) Symplastic communication between primary and developing lateral roots of *Arabidopsis thaliana*. J Exp Bot **46:** 187–197

**Oparka KJ, Viola R, Wright KM, Prior DAM** (1992) Sugar transport and metabolism in the potato tuber. *In* CJ Pollock, J Farrar, AJ Gordon, eds, Carbon Partitioning within and between Organisms, Bios, Oxford, UK, pp 91–114

**Patrick JW, Offler CE** (1996) Post-sieve element transport of photoassimilates in sink regions. J Exp Bot **47:** 1165–1177

**Rhodes JD, Thain JF, Wildon DC** (1996) The pathway for systemic electrical signal conduction in the wounded tomato plant. Planta **200:** 50–57

**Schmitz K, Cuypers B, Moll M** (1987) Pathway of assimilate transfer between mesophyll cells and minor veins in leaves of *Cucumis melo* L. Planta **171:** 19–29

**Tucker EB** (1993) Azide treatment enhances cell-to-cell diffusion in staminal hairs of *Setcreasea purpurea*. Protoplasma **174:** 45–49

**Turgeon R** (1996) Phloem loading and plasmodesmata. Trends Plant Sci **1:** 418–423

**Turgeon R, Beebe DU, Gowan E** (1993) The intermediary cell: minor-vein anatomy and raffinose oligosaccharide synthesis in the Scrophulariaceae. Planta **191:** 446–456

**Turgeon R, Webb JA, Evert RF** (1975) Ultrastructure of minor veins in *Cucurbita pepo* leaves. Protoplasma **83:** 217–232

**Turgeon R, Wimmers LE** (1988) Different patterns of vein loading of exogenous [$^{14}$C]sucrose in leaves of *Pisum sativum* and *Coleus blumei*. Plant Physiol **87:** 179–182

**van Bel AJE** (1996) Interaction between sieve element and companion cell and the consequences for photoassimilate distribution. Two structural hardware frames with associated software packages in dicotyledons? J Exp Bot **47:** 1129–1140

**van Bel AJE, Ammerlaan A, Van Dijk AA** (1994) A three-step screening procedure to identify the mode of phloem loading in intact leaves. Evidence for symplasmic and apoplasmic phloem loading associated with the type of companion cell. Planta **192:** 31–39

**van Bel AJE, Gamalei YV, Ammerlaan A, Bik LPM** (1992) Dissimilar phloem loading in leaves with symplasmic and apoplasmic minor-vein configurations. Planta **186:** 518–525

**van Bel AJE, Kempers R** (1991) Symplastic isolation of the sieve element-companion cell complex in the phloem of *Ricinus communis* and *Salix alba* stems. Planta **183:** 69–76

**van Bel AJE, Kempers R** (1996) The pore/plasmodesm unit; key element in the interplay between sieve element and companion cell. Prog Bot **58:** 278–291

**van Bel AJE, Oparka KJ** (1995) On the validity of plasmodesmograms. Bot Acta **108:** 174–182

**van Bel AJE, Van Rijen HVM** (1994) Microelectrode-recorded development of the symplasmic autonomy of the sieve element/companion cell complex in the stem phloem of *Lupinus luteus* L. Planta **192:** 165–175

**Van der Schoot C, van Bel AJE** (1989) Glass microelectrode measurements of sieve tube membrane potentials in internodes and petioles of tomato (*Solanum lycopersicum*). Protoplasma **149:** 144–154

**Wimmers LE, Turgeon R** (1991) Transfer cells and solute uptake in minor veins of *Pisum sativum* leaves. Planta **186:** 2–12

**Wooding FBP, Northcote DH** (1965) The fine structure and development of the companion cell of the phloem of *Acer pseudoplatanus*. J Cell Biol **24:** 117–128

**Wright KM, Oparka KJ** (1997) Metabolic inhibitors induce symplastic movement of solutes from the phloem pathway of *Arabidopsis* roots. J Exp Bot **48:** 1807–1814